

Giant Helium Dimers Produced by Photoassociation of Ultracold Metastable Atoms

J. Léonard,* M. Walhout,† A. P. Mosk,‡ T. Müller,§ M. Leduc, and C. Cohen-Tannoudji

*Ecole Normale Supérieure and Collège de France
Laboratoire Kastler Brossel, 24 rue Lhomond, 75231 Paris Cedex 05, France*

(Dated: October 25, 2018)

We produce giant helium dimers by photoassociation of metastable helium atoms in a magnetically trapped, ultracold cloud. The photoassociation laser is detuned red of the atomic $2^3S_1 - 2^3P_0$ line and produces strong heating of the sample when resonant with molecular bound states. The temperature of the cloud serves as an indicator of the molecular spectrum. We report good agreement between our spectroscopic measurements and our calculations of the five bound states belonging to a 0_u^+ purely long-range potential well. These previously unobserved states have classical inner turning points of about $150 a_0$ and outer turning points as large as $1150 a_0$.

PACS numbers: 34.20.Cf, 32.80.Pj, 34.50.Gb

In the purely long-range molecules first proposed by Stwalley *et al.* [1], the binding potential depends only on the long-range part of the atom-atom interaction, and the internuclear distance is always large compared with ordinary chemical bond lengths. Theoretical description of these molecules involves only the leading C_3/R^3 terms of the electric dipole-dipole interaction and the fine structure inside each atom. These well-known interactions allow precise calculation of potential wells and rovibrational energies. Previous experimental studies of such spectra in alkali atoms have utilized the technique of laser-induced photoassociation (PA) in a magneto-optical trap (MOT) [2, 3]. In addition to testing calculations of molecular structure, that work has produced precise measurements of excited-state lifetimes [4, 5, 6, 7] and has led to accurate determinations of s-wave scattering lengths for alkali systems, which are of interest for studies of Bose Einstein condensates (BECs)[8, 9].

This letter reports novel spectroscopic measurements and calculations for extraordinarily long-range molecules that are produced when two ^4He atoms in the metastable 2^3S_1 state absorb laser light tuned close to the $2^3S_1 - 2^3P_0$ (D_0) atomic line at $\lambda = 1083$ nm. As compared with the alkali dimers considered previously, the potential wells are shallower, and molecules are much more tenuous, with an internuclear distance reaching values as large as $1150 a_0$ ($a_0 \simeq 0.53 \text{ \AA}$, the Bohr radius). At such large distances, retardation clearly influences the dipole-dipole interaction. Moreover, these purely long-range molecular states of metastable helium are distinctive in that each atom carries a high internal energy (the 2^3S_1 state lies 20 eV above the ground state). While one normally expects Penning ionization to destabilize such

energetic molecules, we note that purely long-range interactions might rather suppress this process, since the atoms are effectively held apart by the same potential that binds them together. The absence of purely long-range resonances in recent PA experiments in Utrecht, which monitored ion production rates in a MOT, is consistent with this reasoning [10].

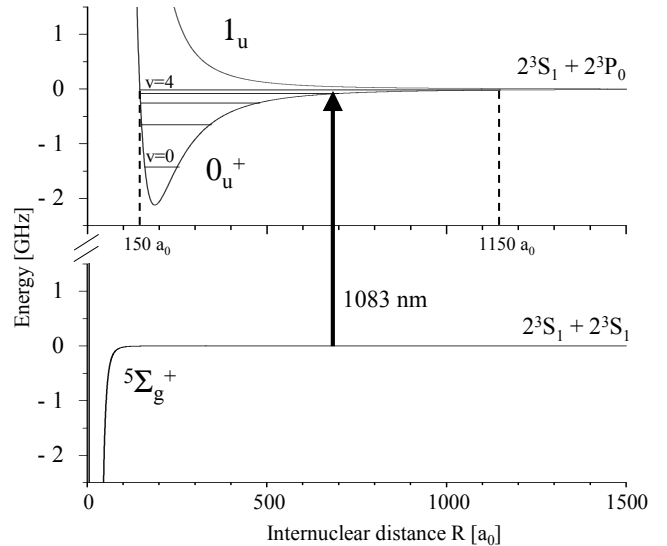


FIG. 1: Molecular potentials involved in the electronic excitation of two 2^3S_1 spin-polarized ^4He atoms. The $5\Sigma_g^+$ potential is taken from [21]. The excited potentials are calculated as described in the text and are the only experimentally accessible potentials linked to the $2^3S_1 + 2^3P_0$ asymptote. Five bound states ($v=0$ to 4) lie in the 0_u^+ well. Their inner turning points are around $150 a_0$, and their outer turning points range from $250 a_0$ ($v=0$) to $1150 a_0$ ($v=4$).

The present experiment differs significantly from reported PA measurements with ^4He in a MOT [11]. Our atomic cloud is confined in a magnetic trap and cooled nearly to the BEC transition [12, 13]. The phase space density is typically six orders of magnitude higher than in a MOT, so the PA process is much more efficient [14].

*Electronic address: leonard@lkb.ens.fr

†Permanent address: Calvin College, Grand Rapids, MI, USA.

‡Permanent address: FOM instituut voor plasmafysica Rijnhuizen, and University of Twente, The Netherlands.

§Present address: Institut für Quantenoptik, Universität Hannover, Germany.

In addition, our magnetically trapped atoms are spin-polarized in a single Zeeman sublevel of the 2^3S_1 state, so the initial quasi-Zeeman state is $^5\Sigma_g^+$. Therefore, only *ungerade* excited states are accessible. Finally, whereas previous PA experiments have monitored only ions or trap losses, we use absorption imaging to detect heating effects in the atomic cloud. Molecular resonances that produce no ions or very little trap loss can still be detected with our method.

Fig. 1 shows the only two potentials that can be excited in our experiment in the vicinity of the D_0 atomic line. The photoassociation experiment consists in driving the transition from free pairs of 2^3S_1 atoms to bound states in the purely long-range 0_u^+ well connected to the $2^3S_1 + 2^3P_0$ asymptote. Measurements of the bound-state spectrum proceed as follows. About 10^9 atoms are trapped in a MOT before being transferred into an Ioffe-Pritchard magnetostatic trap. An evaporative cooling sequence that utilizes RF-induced spin flips cools the atoms to 2-30 μK . The critical temperature for Bose-Einstein condensation is in the range 1 to 4 μK , depending on the density [12, 23].

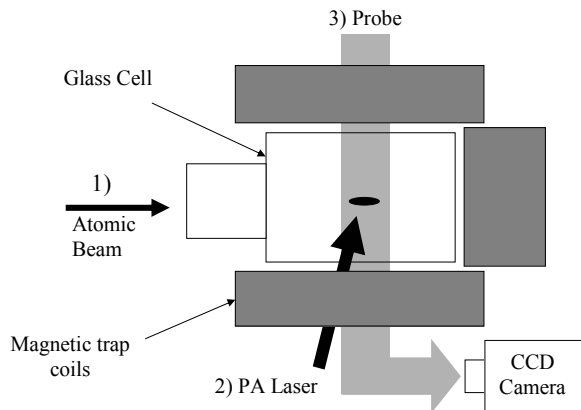


FIG. 2: Experimental setup. 1) Metastable helium atoms are trapped and evaporated down to a few μK and a peak density of order 10^{13} cm^{-3} . 2) The cloud is illuminated inside the magnetic trap by the photoassociation (PA) laser for a few ms. 3) The cloud is released and imaged on a CCD camera after ballistic expansion.

After cooling, the cloud is illuminated for a few ms by light from a “PA laser” beam containing all polarization components relative to the magnetic field axis. Just after this PA pulse, the cloud is released and then detected by means of destructive absorption imaging after ballistic expansion. The number of atoms, the peak optical density, and the temperature are thereby measured as functions of the PA laser frequency. Fig. 3 shows the optical density after contributions from atomic (D_0) absorption have been subtracted. For this broad scan, the PA laser is a temperature-controlled diode laser with a 3-MHz spectral width. A Fabry-Perot cavity is used to measure the frequency relative to a reference laser frequency locked to the $2^3S_1 - 2^3P_2$ atomic line. The accuracy of the PA frequency in this case is 10 MHz.

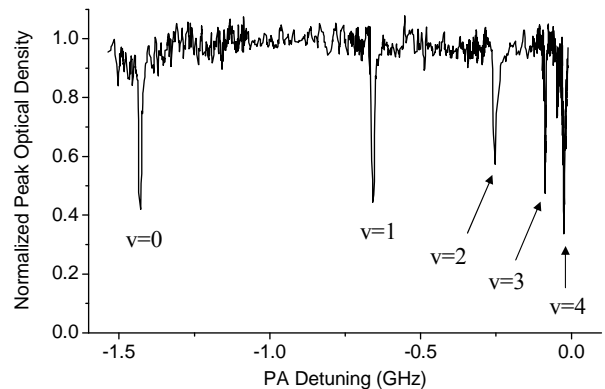


FIG. 3: Experimental data. The peak optical density is plotted versus PA laser detuning, measured with respect to the $2^3S_1 - 2^3P_0$ atomic transition. We have subtracted a Lorentzian-shaped background loss due to atomic absorption and divided by a signal proportional to the number of atoms in the trap, yielding a “normalized” peak optical density signal. Each line has been probed separately with different laser intensities and exposure time ranging from (0.1 μW ; 20 ms) to (100 μW ; 200 ms). Therefore the relative depths of the five lines are not relevant.

More accurate spectroscopy is performed with a PA beam derived from a cavity-stabilized laser (width 0.3 MHz) locked to the D_0 line. The PA beam is tuned to the molecular lines by acousto-optic modulators. Its intensity is set between 0.01 and 1 mW/cm^2 , and the exposure time between 0.1 and 10 ms. With this technique we can reach and zoom in on the four highest ($v=1$ to $v=4$) lines in the 0_u^+ well. Fig. 4 shows typical experimental data for the line $v=4$. Figs. 4a) and 4b) demonstrate that the peak optical density drops significantly when the PA beam is resonant with a molecular line, even if trap loss is weak. This situation is explained by the strong heating indicated in Fig. 4c. The temperature increase provides a very sensitive diagnostic for resonances that produce little loss. Assuming that the heat deposited in the cloud is proportional to the number of molecules produced, we fit the frequency dependence of the temperature to a Lorentzian curve. The FWHM of the molecular lines is measured at low intensities to be 3.0(3) MHz, within the expected range for the molecular radiative width ($\Gamma_{mol} \leq 2\Gamma$).

The heating mechanism that produces our signals can be roughly understood as follows. After absorbing a photon near the outer turning point, the molecular system can decay radiatively into two fast metastable atoms, each with a non-zero probability of being in the trapped state. Since the trap depth is 15 mK, fast atoms can remain trapped and heat up the whole cloud. This reasoning is supported by the fact that we can convert the heating into trap loss if, during a 10 ms thermalization time after the PA pulse, we apply an RF “knife” that removes fast atoms from the trap. The simultaneous measurement of small trap loss and significant temperature increase suggests that each molecular excitation heats the

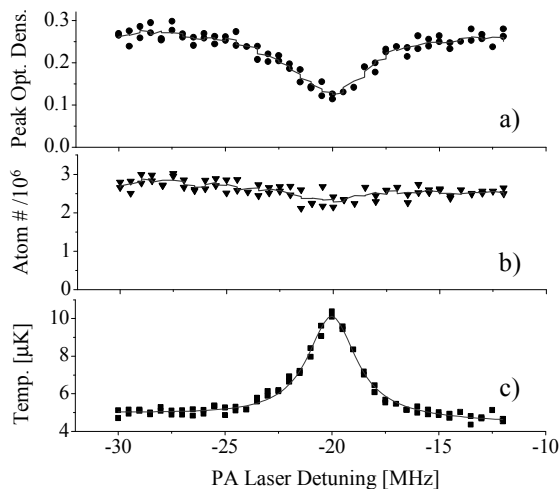


FIG. 4: Detection of the line $v=4$ in the 0_u^+ potential well. a) Peak optical density, b) atom number and c) temperature in μK versus PA laser frequency. Each point represents a new evaporated cloud after PA pulse illumination and ballistic expansion. The curves in graphs a) and b) indicate the averaging of data over 5 adjacent points. The curve in graph c) is a Lorentzian fit to the data.

sample considerably. This is the reason why the temperature probe is so sensitive.

We measure the detuning $\delta < 0$ of the PA laser relative to the D_0 atomic line. The initial 2^3S_1 pair undergoes an inhomogeneous Zeeman effect due to the trapping potential. Additionally, the relative kinetic energy of the pair is characterized by a non-zero temperature T . Each of these effects contributes a $\frac{3}{2}k_B T$ Boltzmann term to the initial average energy of a pair. Hence, the binding energy $hb < 0$ of a given vibrational state is $hb = h\delta + 2\mu B_0 + 3k_B T$, where $2\mu B_0 > 0$ is the Zeeman shift for a 2^3S_1 pair at the center of the trap. Additional recoil and mean-field shifts of order 10 kHz are neglected because they are much smaller than our experimental uncertainty. Each line is probed in different conditions of T (2 - 30 μK), B_0 (300 mG - 10 G) and density (10^{12} - $5 \times 10^{13} \text{ cm}^{-3}$). Within the accuracy of our experiment we finally find no density or magnetic-field dependence of the binding energies, and for each line we estimate an uncertainty of ± 0.5 MHz. Given this uncertainty and the range of magnetic field explored, we can infer an upper limit for the 0_u^+ magnetic moment of ~ 0.04 Bohr magnetons [24].

In order to interpret the experimental frequency spectrum quantitatively, we calculate the coupling between the atomic orbitals of one atom in the 2^3S_1 state and another in the $2^3P_{J=0,1,2}$ state, which involves 54 molecular potentials. This coupling is constructed as a perturbative Hamiltonian in the basis of fine-structure-free atomic states. At large internuclear distances R , the lowest-order term of the electromagnetic interaction is the retarded dipole-dipole interaction [15, 16], which is fully determined by the coefficient $C_3 = (3/4)\hbar\Gamma/k^3$, where

$\Gamma = 2\pi \times 1.6248$ MHz [17] is the atomic linewidth, and $k = 2\pi/\lambda$ is the wave number. This interaction includes no coupling between electronic orbital and spin angular momenta (\vec{L} and \vec{S}) and is diagonal in the molecular Hund's case (a) basis.

In the absence of \vec{L} - \vec{S} coupling, the potential curves resulting from dipole-dipole interaction are purely attractive or repulsive and have a single asymptote. When we include the atomic fine structure in the Hamiltonian [18], the coupling gives rise to three distinct asymptotes and to anti-crossings between attractive and repulsive curves, leading to purely long-range potential wells [25]. We construct the fine-structure coupling phenomenologically from 2^3P splittings that have been measured accurately [19, 20]. If there is no rotation, only the projection Ω of the total electronic angular momentum on the molecular axis remains a good quantum number. Our experiment probes the 0_u^+ purely long-range well plotted in Fig. 1.

We also consider how the rotation of the molecule can couple electronic states ($\Delta\Omega = 0, \pm 1$), an effect that will leave $\Omega = 0$ and 0_u^+ as only approximate labels. Ultimately, only the total angular momentum J remains a good quantum number. Our final addition to the Hamiltonian is the operator $\vec{\ell}^2/(2\mu R^2)$ [22], where $\vec{\ell} = \vec{J} - \vec{L} - \vec{S}$ is the nuclear angular momentum operator. In the s-wave scattering regime, the initial ($2^3S_1 + 2^3S_1$) pair exists only in the $J = 2$ state. Elementary group theory and Bose-Einstein statistics for the nuclei [22] dictate that J in the excited state must be odd, namely 1 or 3. What is more, the Condon radius at which the transition occurs is so large that the excited molecule is in almost the same quantum state as a non-interacting pair of atoms in the $2^3S_1 + 2^3P_0$ state (Hund's case (c)). Therefore $J = 1$ is dominant.

The Hamiltonian including retarded dipole-dipole interaction, fine structure, and nuclear rotation is diagonalized numerically. The 0_u^+ well cited above is found to remain almost pure; that is, the couplings to other Ω subspaces are very small. It is 2 GHz deep and contains 5 bound states (see Fig. 1). The inner turning points of these bound states are around $150 a_0$ and the outer turning point is as large as $1150 a_0$ for the $v=4$ vibrational state. From the discussion above, it is clear that even the repulsive, inner part of the potential has purely long-range character; this fact distinguishes these dimers from those bound by usual chemical interactions. The large internuclear distance is also the reason why the next-order term in C_6/R^6 of the electromagnetic interaction is negligible [26]. More detail about the theoretical approach will be given in a forthcoming paper [27].

Measured and calculated binding energies in the 0_u^+ well are presented in Table I. The measured spectrum agrees very well with the predicted $J=1$ progression, except for $v=1$, for which the 2 MHz discrepancy remains unexplained. Although it is too weak to be observed, the $J = 3$ progression has been calculated to illustrate the expected rotational splitting. Finally, comparison with calculated results for a non-retarded dipole-dipole

TABLE I: Measured and calculated binding energies in the 0_u^+ well. The first column gives the experimental results. Vibrational states $v=1$ to $v=4$ are measured with a 0.5 MHz uncertainty, $v=0$ with a 10 MHz uncertainty. The next two columns give calculations following the model described in the text for $J = 1$ with and without including retardation effects. The last column contains calculated $J = 3$ results with retardation.

	Experiment	$J = 1$	$J = 1^a$	$J = 3$
$v=4$	-18.2(5)	-18.250	-16.646	—
$v=3$	-79.6(5)	-79.555	-76.933	-41.761
$v=2$	-253.3(5)	-253.27	-249.47	-175.14
$v=1$	-648.5(5)	-650.37	-645.27	-513.39
$v=0$	-1430(10)	-1425.6	-1419.1	-1220.0

^aCalculated while neglecting retardation effects

interaction demonstrates the significant influence of retardation. We note that our measurement confirms the assumed value of C_3 to within 0.3%.

In related work, we have measured other molecular lines, not belonging to purely long-range potentials, to the red of $2^3S_1 + 2^3P_2$. Their identification is under way. Additionally, an accurate measurement of the heat deposited in the cloud by decaying long-range molecules is in development; this could lead to a quantitative

“calorimetric” method of measuring PA rates and thermal transport properties in the sample. Finally, this letter provides a foundation for a two-color, stimulated Raman experiment that would prepare molecules in the most weakly bound state of the $^5\Sigma_g^+$ potential shown in Fig. 1, with the 0_u^+ , $v=0$ state as an intermediate state. The corresponding Franck-Condon factor of ~ 0.1 suggests that the transition rate should be high. The lifetime of these atypical dimers formed from two 2^3S_1 metastable atoms is unknown. Moreover, an accurate measurement of the s-wave elastic scattering length of 2^3S_1 helium should follow directly from the measured binding energy [8].

Acknowledgements : The authors thank Peter van der Straten (Utrecht), the Cold Atoms and Molecules group at Laboratoire Aimé Cotton and the Cold Atoms group at Laboratoire Kastler Brossel for fruitful discussions. The work of APM is part of the research program of *Stichting voor Fundamenteel Onderzoek der Materie* (FOM) which is financially supported by *Nederlandse Organisatie voor Wetenschappelijk Onderzoek* (NWO). MW was partly funded by National Science Foundation Grant PHY-0140135, and TM by the *Procope* exchange program.

-
- [1] W.C. Stwalley, Y.-H. Uang, G. Pichler, Phys. Rev. Lett. **41**, 1164 (1978).
- [2] P. D. Lett, P.S. Julienne, W.D. Phillips, Annual Rev. Phys. Chem. **46**, 423 (1995).
- [3] R.A. Cline, J.D. Miller, D.J. Heinzen, Phys. Rev. Lett. **73**, 632 (1994).
- [4] W.I. McAlexander, E.R.I. Abraham, R.G. Hulet, Phys. Rev. A **54**, R5 (1996).
- [5] K. M. Jones, P. S. Julienne, P. D. Lett, W. D. Phillips, E. Tiesinga, C. J. Williams, Europhys. Lett. **35**, 85 (1996).
- [6] H. Wang, J. Li, X. T. Wang, C. J. Williams, P. L. Gould, W. C. Stwalley, Phys. Rev. A **55**, R1569 (1997).
- [7] R.F. Gutterres, C. Amiot, A. Fioretti, C. Gabbanini, M.Mazzoni, O. Dulieu, Phys. Rev. A **66**, 024502 (2002).
- [8] E. R. I. Abraham, W. I. McAlexander, C.A. Sackett, R. G. Hulet, Phys. Rev. Lett. **74**, 1315 (1995).
- [9] J. R. Gardner, R. A. Cline, J. D. Miller, D. J. Heinzen, H. M. J. M. Boesten, B. J. Verhaar, Phys. Rev. Lett. **74**, 3764 (1995).
- [10] P. van der Straten, private communication.
- [11] N. Herschbach, P. J. J. Tol, W. Vassen, W. Hogervorst, G. Woestenenk, J.W. Thomsen, P. van der Straten, A. Niehaus, Phys. Rev. Lett. **84**, 1874, (2000).
- [12] F. Pereira Dos Santos, J. Léonard, Junmin Wang, C. J. Barrelet, F. Perales, E. Rasel, C. S. Unnikrishnan, M. Leduc, C. Cohen-Tannoudji, Phys. Rev. Lett. **86**, 3459 (2001).
- [13] A. Robert, O. Sirjean, A. Browaeys, J. Poupard, S. Nowak, D. Boiron, C. I. Westbrook, A. Aspect, Sci. Mag. **292**, 463 (2001).
- [14] P. Pillet, A. Crubellier, A. Bleton, O. Dulieu, P. Nosbaum, I. Mourachko, F. Masnou-Seeuws, J. Phys. B **30**, 2801 (1997).
- [15] E.I. Dashevskaya, A.I. Voronin, E.E. Nikitin, Can. J. Phys. **47**, 1237 (1969).
- [16] W. J. Meath, J. Chem. Phys. **48**, 227 (1968).
- [17] G. W. F. Drake in *Atomic, Molecular and Optical Physics Handbook*, edited by G. W. F. Drake, AIP Press, Chap.11 (1996).
- [18] M. Movre and G. Pichler, J. Phys. B, **10**, 2631 (1977).
- [19] M.C. George, L.D. Lombardi, E.A. Hessels, Phys. Rev. Lett. **87**, 173002, (2001), and references therein.
- [20] J. Castilleja, D. Livingston, A. Sanders, D. Shiner, Phys. Rev. Lett. **84**, 4321, (2000), and references therein.
- [21] J. Stårck, W. Meyer, Chem. Phys. Lett. **225**, 229, (1991).
- [22] J. T. Hougen, Nat. Bur. Stand. (U.S.), Monograph 115 (1970).
- [23] F. Pereira dos Santos, J. Leonard, Junmin Wang, C. J. Barrelet, F. Perales, E. Rasel, C. S. Unnikrishnan, M. Leduc, C. Cohen-Tannoudji, Eur. Phys. J. D, **19**, 103 (2002).
- [24] Since pure 0_u^+ states are not degenerate, only molecular rotation gives rise to a magnetic moment, which is therefore expected to be of the order of the nuclear magneton.
- [25] The absence of hyperfine structure in ^4He leads to relatively simple molecular potentials.
- [26] We estimate the C_6/R^6 correction is at least 4 orders of magnitude smaller than C_3/R^3 for an internuclear distance larger than $150 a_0$.
- [27] The calculation exhibits two other ungerade purely long-range wells connected to the $2^3S_1 + 2^3P_1$ asymptote. They are even shallower and support fewer bound states than the well examined here. Their inner turning points are over $300 a_0$.